Pulmonary vein to ganglionated plexi distance predicts cryoballoon ganglionated plexi modification

Kenji Yamaji, MD, PhD,[1] Mayu Kako, MD,[1] Kota Fujihara, MD,[1] Yuto Fukawa, MD,[1] Naoya Takahashi, MD,[1] Eiichiro Nakagawa, MD,[1] Ryobun Yasuoka, MD, PhD,[2] Masahiro Yoshinaga, MD,[1] Masahiro Karakawa, MD, PhD[1]

From the [1]Department of Cardiology, Osaka Prefecture Saiseikai Izuo Hospital, Osaka, Japan, and [2]Department of Cardiology, Kindai University Hospital, Osaka, Japan.

BACKGROUND Cryoballoon ablation (CBA) for atrial fibrillation (AF) can cause incidental modification of ganglionated plexi (GP), which may contribute to arrhythmia control; however, the anatomic factors associated with GP modification remain poorly understood.

OBJECTIVE We investigated the relationship between the distance from the pulmonary vein–left atrial (PV–LA) junction to GP sites and GP modification during CBA using voltage mapping.

METHODS This retrospective study analyzed 50 patients with paroxysmal AF undergoing CBA. Preprocedural computed tomography images were integrated into a 3-dimensional electroanatomic mapping system to measure PV–LA junction to GP (PV–GP) distances. GP modification was defined as voltage attenuation at GP sites after ablation. Receiver operating characteristic analysis was performed to assess predictive performance.

RESULTS GP modification occurred more frequently at sites located closer to the PV–LA junction. Upper GP regions demonstrated higher modification rates than lower regions, and PV–GP distance showed reasonable discrimination for predicting GP modification.

CONCLUSION Anatomic proximity between the PV–LA junction and GP seems to be a key determinant of GP modification during CBA. Quantitative assessment of PV–GP distance may help predict autonomic effects and support optimization of AF ablation strategies.

KEYWORDS Atrial fibrillation; Cryoballoon ablation; Pulmonary vein isolation; Ganglionated plexi; Autonomic nervous system modulation

(Heart Rhythm O^2 2026;■:1–9)

Introduction

Atrial fibrillation (AF) is associated with increased morbidity and mortality.[1,2] Since Haïssaguerre et al[3] demonstrated pulmonary vein (PV) triggers, PV isolation has become the cornerstone for catheter ablation. Cryoballoon ablation (CBA) has been widely adopted for its efficiency and safety.[4–6] Ganglionated plexi (GPs) within the left atrium (LA) are important modulators of AF initiation and maintenance.[7–9] Autonomic changes often precede AF episodes,[10,11] and GP clusters are generally distributed in 5 regions: the superior left GP (SLGP), anterior right GP (ARGP), Marshall tract GP (MTGP), inferior right GP (IRGP), and inferior left GP (ILGP) (Figure 1). These sites can be identified by high-frequency stimulation (HFS).[12–15] Previous studies have demonstrated that GP ablation improves arrhythmia outcomes.[9,16–18] HFS is technically demanding and may induce bradycardia and hypotension.[7,16] Anatomically guided ablation using electroanatomic mapping has been proposed as an alternative.[9,16,19] Although incidental GP modification often occurs during CBA, its anatomic determinants, particularly the role of distance from the PV–LA junction to GP (PV–GP distance), remain inadequately explored.[20–23] Voltage mapping has emerged as an objective modality for assessing GP modification.[24,25] Therefore, we evaluated the relationship between PV–GP distance and incidental GP modification using the EnSite NavX system (Abbott, St. Paul, MN) and pre- and postablation voltage mapping in 50 patients with paroxysmal AF. Voltage mapping was also compared with HFS in 28 patients to assess its potential as an alternative. These findings provide a practical reference for centers not performing HFS and may help refine strategies beyond standard CBA.

Address reprint requests and correspondence: Dr Kenji Yamaji, Department of Cardiology, Osaka Prefecture Saiseikai Izuo Hospital, 3-4-5 Kitamura, Taisho-ku, Osaka City, Osaka 551-0032, Japan. E-mail address: yamajijunnai@yahoo.co.jp.

2666-5018/

https://doi.org/10.1016/j.hroo.2026.05.005

KEY FINDINGS

- Pulmonary vein–ganglionated plexi distance was strongly associated with successful ganglionated plexi modification during cryoballoon ablation.
- Ganglionated plexi located close to the pulmonary vein–left atrial junction were frequently modified by cryoballoon ablation, whereas those located farther from the junction were less likely to be modified.
- Postablation voltage mapping showed high concordance with high-frequency stimulation in the validation subgroup, suggesting that it may provide an objective method for evaluating ganglionated plexi modification.

Methods

Study design and population

This single-center, retrospective study included 50 consecutive patients with paroxysmal AF who underwent CBA between September 2017 and April 2020 at Osaka Prefecture Saiseikai Izuo Hospital. All patients underwent preprocedural contrast-enhanced computed tomography (CT). A 3-dimensional LA geometry was created using EnSite NavX and fused with the preprocedural CT model. GP sites were functionally identified by HFS and tagged on the integrated electroanatomic map; they were not directly identified on CT alone. The shortest distance from the PV–LA junction to each HFS-defined GP site was measured on the integrated model as a post hoc analysis. CT was used as an anatomic reference to support distance measurements. The study protocol was reviewed and approved by the Ethics Committee of Osaka Prefecture Saiseikai Izuo Hospital on August 19, 2024, and an informed consent was obtained through an opt-out process in accordance with institutional and national ethics guidelines. No formal approval number was issued for this retrospective study.

Ablation procedure

All procedures were performed via right femoral venous access under general anesthesia. After performing a transseptal puncture, a second- or fourth-generation 28-mm cryoballoon (Arctic Front Advance™ or Arctic Front Advance Pro™, Medtronic, Minneapolis, MN) was deployed together with a mapping catheter (Achieve™ mapping catheter, Medtronic). All PVs (left superior, left inferior, right superior, and right inferior) were targeted for electrical isolation. Balloon positioning and complete occlusion were confirmed via contrast injection. Freezing applications were typically delivered for 180 seconds. If isolation was not achieved, the balloon position was adjusted, and an additional application was administered. To ensure safety, esophageal temperature monitoring and phrenic nerve pacing were routinely performed.[4]

Preablation GP mapping and HFS

Before CBA, a 10-pole ring catheter (EPstar Libero™, Japan Lifeline, Tokyo, Japan) was used to construct a detailed map of the LA within the EnSite NavX system and fused with the preprocedural CT model.[26] HFS was then delivered to suspected GP sites using a radiofrequency (RF) ablation catheter (CoolPath™, Abbott) under the following settings: 20 Hz, 10 V, and 2 ms. A positive GP response was defined as a >50% reduction in heart rate or the occurrence of ≥2 atrioventricular blocks within 10 seconds.[15]

Tagging of GP sites

HFS-positive and HFS-negative sites were annotated using color-coded tags within the EnSite system[15,18]

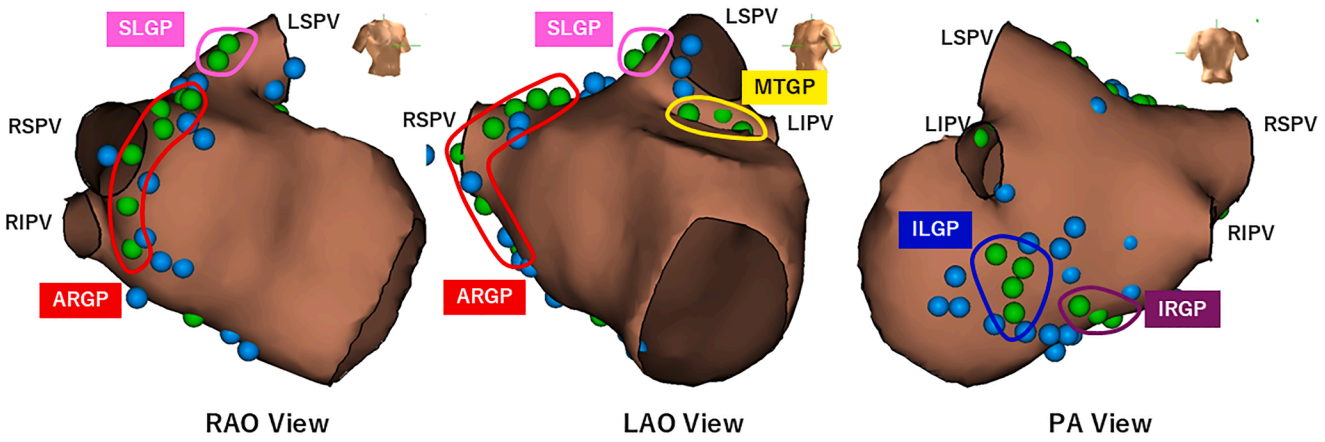

Figure 1 Distribution of HFS-defined GPs and anatomic relationship in a representative case. The distribution of GPs identified by HFS before ablation is shown on a left atrial model in a representative case. *Green dots* indicate HFS-positive sites, and *blue dots* indicate HFS-negative sites. These distributions are overlaid on the 5 conventionally described GP regions (ARGP, SLGP, MTGP, IRGP, and ILGP), which are indicated by *colored outlines*. This figure is intended as a visual reference to show the relationship between HFS-defined GP sites and anatomic classification. *Red*, ARGP; *pink*, SLGP; *yellow*, MTGP; *blue*, ILGP; *purple*, IRGP. ARGP = anterior right GP; GP = ganglionated plexus; HFS = high-frequency stimulation; ILGP = inferior left GP; IRGP = inferior right GP; LAO = left anterior oblique; LIPV = left inferior pulmonary vein; LSPV = left superior pulmonary vein; MTGP = Marshall tract GP; PA = posteroanterior; RAO = right anterior oblique; RIPV = right inferior pulmonary vein; RSPV = right superior pulmonary vein; SLGP = superior left GP.

(Figures 1 and 2A). Each tag was set to a diameter of 4 mm to ensure precise recording of anatomic locations, thereby creating a detailed 3-dimensional distribution map of HFS-defined GP sites.

Postablation evaluation

After confirming complete PV isolation by demonstrating both entrance and exit block, another round of voltage mapping was performed. Voltage was then measured at each preablation HFS-positive site (Figure 2C and 2D). In a subset of 28 patients, HFS was repeated after ablation at the same sites to validate the voltage-based definition of GP modification.

Additional ablation procedures, including cavotricuspid isthmus ablation and roof line ablation, were performed only after completion of GP modification assessment.

GP location identification

The following 5 GP regions (SLGP, ARGP, MTGP, IRGP, and ILGP) were analyzed.[15] For subsequent analyses, these regions were categorized into upper (SLGP, ARGP, and MTGP) and lower GPs (IRGP and ILGP) based on their anatomic relationship with the PV–LA junction. Upper GPs are located adjacent to the superior and anterior aspects of the PV–LA junction, whereas lower GPs are positioned along the inferior–posterior wall of the LA.

PV–GP distance was defined as the shortest distance from the PV–LA junction to each HFS-defined GP tag on the integrated EnSite–CT model.

Definition of GP modification

The primary endpoint of this study was GP modification after CBA based on postablation voltage mapping at HFS-positive sites (Figure 2D). Sites were classified as "modified" when their postablation bipolar voltage was <0.05 mV, indicating complete local attenuation.[27] In contrast, sites with preserved voltage (≥ 0.05 mV) were classified as "non-modified." This binary classification provided the basis for subsequent analyses, including receiver operating characteristic (ROC) curve analysis and multivariate logistic regression.

Concordance between HFS and voltage mapping

Concordance between postablation HFS and voltage mapping was assessed in the 28-patient validation subgroup. Concordance was defined as either loss of the HFS response with a postablation voltage of <0.05 mV or a persistent HFS response with preserved voltage of ≥ 0.05 mV. Concordance rates were calculated using postablation HFS findings as the functional reference.

Statistical analysis

All statistical analyses were performed using JMP version 14.0 (SAS Institute Inc, Cary, NC). Continuous variables were expressed as means ± standard deviations or medians with interquartile ranges (IQRs), as appropriate. Normality was assessed using the Shapiro-Wilk test. Categorical variables were summarized as counts and percentages. For each GP, the HFS positivity rate, mean PV–GP distance, and GP modification rate after CBA were calculated. Distances were compared using 1-way analysis of variance with Tukey's post hoc test. Distances of modified vs nonmodified GP sites were compared using *t* test or Mann-Whitney U test depending on the data distribution. Spearman's correlation coefficients were calculated for distance and modification rates. ROC curves were created to evaluate the ability of PV–GP distance to predict voltage loss. The area under the curve (AUC), cutoff values, sensitivity, specificity, positive predictive value, and negative predictive value were calculated. Logistic regression was used to identify predictors of GP modification. The multivariate models included PV–GP distance, LA volume, age, and $CHADS_2$ score (model 1, distance + LA volume; model 2, distance + LA volume + age; model 3, distance + LA volume + age + $CHADS_2$). Concordance rates between HFS and voltage mapping were then calculated in 28 patients. Fisher's exact test was used for group comparisons. All tests were 2 sided, with $P < .05$ indicating statistical significance. Bonferroni correction was applied for multiple comparisons.

The central illustration summarizes the study design and the relationship between PV–GP distance and GP modification.

Results

Patient characteristics

This study enrolled 50 patients (mean age 69.1 ± 9.1 years; 27 males [54%]; mean body mass index, 23.6; IQR 21.6–26.7 kg/m^2). The mean LA diameter measured via echocardiography was 37.2 ± 3.4 mm, whereas the mean LA volume measured using CT was 91.1 ± 25.9 mL. The median $CHADS_2$ score was 1 (IQR 1–2) (Table 1).

Distribution and ablation outcomes of GP sites

The approximate anatomic distribution of the GP sites identified through HFS before ablation is presented in Figure 1. Based on voltage mapping, we evaluated whether HFS-positive GP sites demonstrated voltage loss (ablation success) after standard CBA (Figure 2C and 2D). Across all GP sites, the mean PV–GP distance was significantly longer for lower GP regions than for the upper GP regions ($P < .001$). The mean PV–GP distances and the corresponding ablation success rates for each GP are discussed in the following subsections.

Upper GP

For the upper GP regions, the mean PV–GP distance and modification rates were as follows: SLGP (6.59 mm; success rate 86.1%), ARGP (7.31 mm; success rate 83.4%), and MTGP (0.78 mm; success rate 93.7%) (Table 2). These sites were located close to the PV orifices, which allowed for adequate coverage by standard CBA energy and induced high modification rates. In particular, the MTGP exhibited the shortest distance (<1 mm) and the highest success rate.

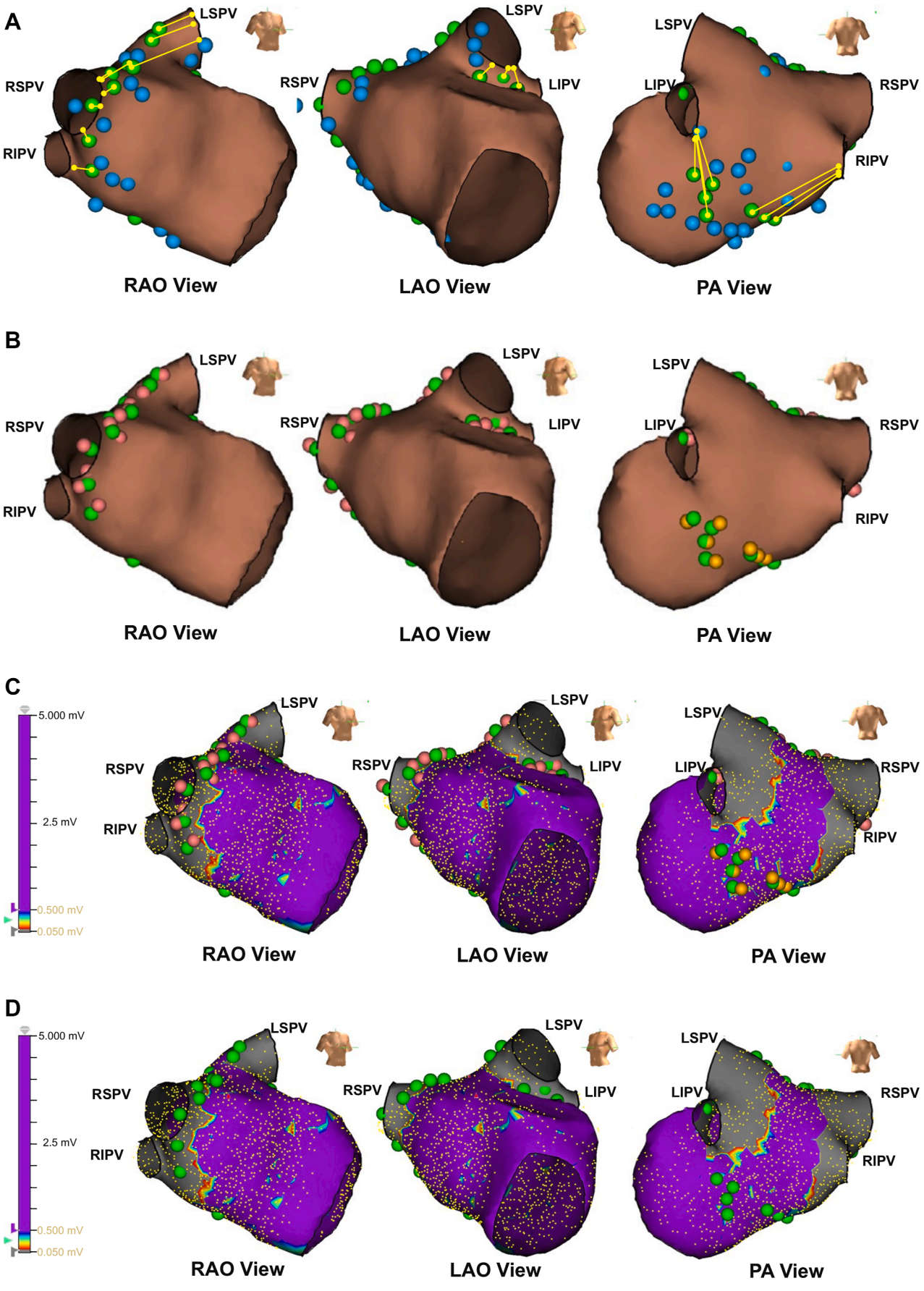
A
LSPV
RSPV
RIPV
LIPV
RAO View
LAO View
PA View
B
C
5.000 mV
2.5 mV
0.500 mV
0.050 mV
D

Table 1 Patient characteristics and baseline data

Characteristic	Value
Demographics	
Age, y	69.1 ± 9.1
Men	27 (54.0)
Weight, kg	62.3 ± 10.9
Height, cm	160.1 ± 9.7
BMI, kg/m^2	23.6 [21.6–26.7]
$CHADS_2$ score	1 [1–2]
Admission vitals	
Systolic blood pressure, mm Hg	129.2 ± 16.4
Diastolic blood pressure, mm Hg	86.0 ± 11.4
Heart rate, beats/min	79.2 ± 11.4
Arrhythmia history	
History of electrical cardioversion	0 (0)
Pacemaker implantation	1 (2.0)
ICD implantation	0 (0)
Baseline ECG: sinus rhythm	47 (94.0)
Medical history	
Hypertension	24 (48.0)
Diabetes mellitus	7 (14.0)
History of heart failure episodes	3 (6.0)
Echocardiographic findings	
Left atrial diameter, mm	37.2 ± 3.4
Left ventricular ejection fraction, %	65.1 ± 5.2
Computed tomography findings	
Left atrial volume, mL	91.1 ± 25.9
Preprocedural laboratory findings	
Hemoglobin, g/dL	13.4 ± 1.4
Creatinine, μmol/L	77.0 ± 22.7
eGFR, mL/min/1.73 m^2	63.0 ± 17.0
BNP, pg/mL	47.75 [27.9–106.5]
Procedural parameters	
Cryoballoon ablation total area, cm^2	12.4 ± 5.3

Clinical characteristics of the 50 patients with paroxysmal atrial fibrillation who underwent cryoballoon ablation. Continuous variables are expressed as mean ± standard deviation or median [interquartile ranges], as appropriate, and categorical variables as numbers (%).

BMI = body mass index; BNP = brain natriuretic peptide; $CHADS_2$ = congestive heart failure, hypertension, age, diabetes mellitus, and stroke/transient ischemic attack; ECG = electrocardiogram; eGFR = estimated glomerular filtration rate; ICD = implantable cardioverter-defibrillator.

Considering modification was uniformly high irrespective of distance, the variability in outcomes was insufficient, with the ROC curve analysis failing to demonstrate predictive value (Figure 3).

Lower GP

The lower GP regions had substantially longer mean PV–GP distances than did the upper GP regions, with the IRGP located at 19.07 mm and showing a success rate of only 12.3% and the ILGP located at 21.3 mm with a success rate of 4.7% (Table 2). These GPs were situated farther from the PV orifices, where incidental modification by CBA was markedly limited. In particular, GP sites located more than 10 mm from the PV–LA junction were rarely modified by CBA alone.

Table 2 Relationship between pulmonary vein–GP distance and cryoballoon ablation response by GP region

GP region	Pre-CBA positive sites (n)	Mean distance (mm)	Post-CBA positive sites (n)	Negative conversion rate (%)
SLGP	108	6.59	15	86.1
ARGP	205	7.31	34	83.4
MTGP	63	0.78	4	93.7
IRGP	122	19.07	107	12.3
ILGP	85	21.3	81	4.7

Distribution of GP sites by anatomic region in 50 patients. For each GP region, the number of high-frequency stimulation-positive sites before cryoballoon ablation, the mean pulmonary vein–GP distance, and the proportion of sites showing loss of responsiveness after ablation are presented.

ARGP = anterior right GP; CBA = cryoballoon ablation; GP = ganglionated plexus; ILGP = inferior left GP; IRGP = inferior right GP; MTGP = Marshall tract GP; SLGP = superior left GP.

Predictive ability of the PV–GP distance based on ROC curve analysis

ROC curve analysis found that an overall cutoff of 11 mm was optimal for predicting GP modification (AUC 0.94; sensitivity 90.4%; specificity 83.0%; positive predictive value 88.3%; negative predictive value 85.8%; Youden's index 0.73; $P < .001$) (Figure 3). According to anatomic site, the cutoff values were 7.5 and 8.0 mm for ARGP and SLGP, respectively, with a combined threshold of 9.0 mm for upper GP (AUC 0.84). In contrast, lower GP demonstrated larger cutoff values than did the upper GP (ie, 19 and 20 mm for IRGP and ILGP, respectively), yielding a combined threshold of 13 mm (AUC 0.94). SLGP achieved an AUC approaching 1.0, whereas MTGP showed no predictive ability (AUC 0.47; $P = .962$).

Concordance between HFS and voltage mapping

In the latter 28 patients, concordance between functional GP evaluation by HFS and voltage mapping was assessed. A total of 415 GP sites were evaluated, and 397 sites showed concordant results (95.7%) (Figure 2C and Table 3). Concordance rates by GP site were as follows: ARGP, 90.5% (124

Figure 2 Distribution, modification, and voltage-HFS concordance of GPs. GPs identified by HFS were visualized using the EnSite system in relation to cryoballoon ablation. **A:** GP sites detected by HFS, with the shortest PV–GP distance indicated by yellow lines. *Blue markers* indicate HFS-negative sites, and *green markers* indicate HFS-positive sites before ablation. **B:** Changes in HFS responsiveness before and after ablation, with persistent positivity shown in *yellow* and loss of response in *pink*. **C:** Postablation voltage mapping overlaid with HFS findings in 28 patients. Low-voltage areas (<0.05 mV), representing GP modification, are shown in *gray*, whereas sites with preserved electrograms are shown in *purple*. **D:** Classification of GP modification based on postablation voltage criteria at preablation HFS-positive GP sites and corresponding HFS responses. CBA = cryoballoon ablation; GP = ganglionated plexus; HFS = high-frequency stimulation; LA = left atrium; LAO = left anterior oblique; PA = posteroanterior; PV = pulmonary vein; PV–LA junction = pulmonary vein–left atrium junction; RAO = right anterior oblique.

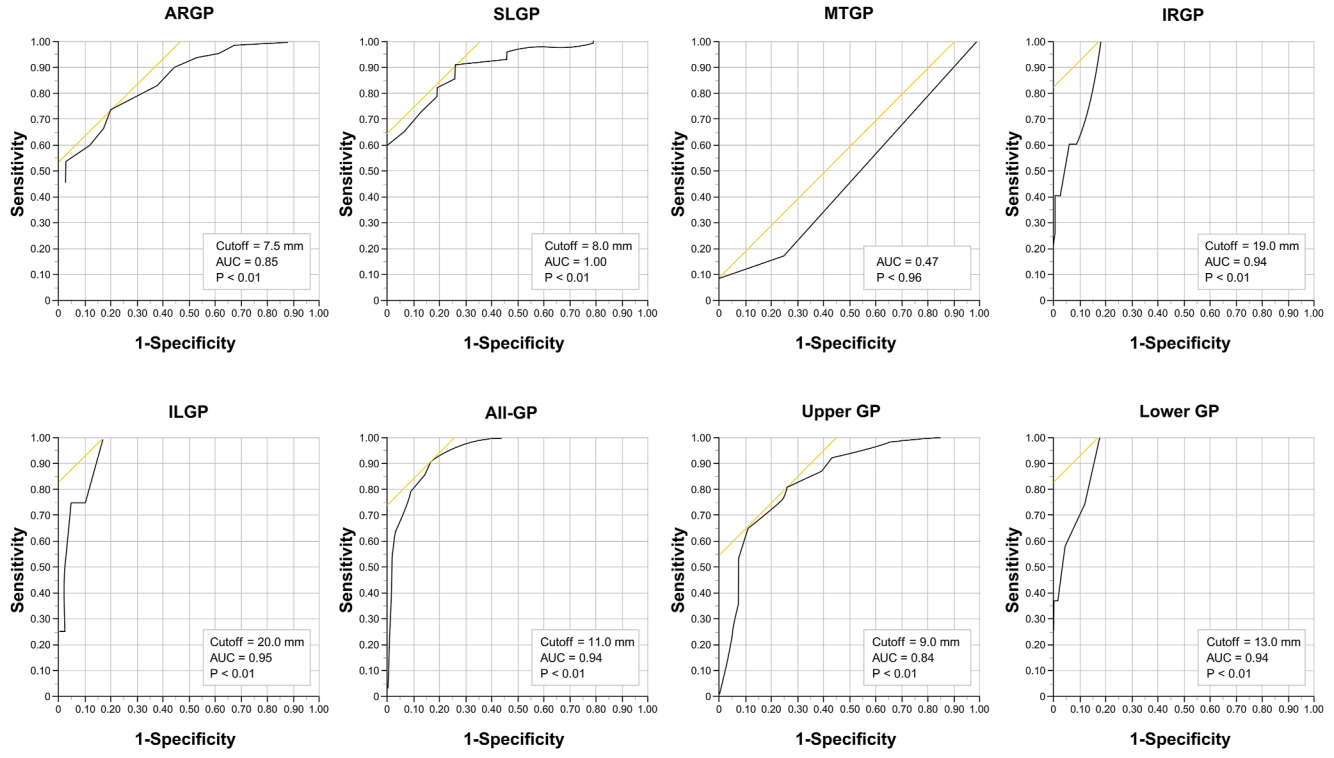

Figure 3 Diagnostic performance of ROC analysis. ROC curves were generated to evaluate the association between the distance between the PV and the GP (PV–GP) and GP modification. Analyses were performed as follows: for all GP sites combined, for the upper GP (SLGP, ARGP, and MTGP), for the lower GP (IRGP and ILGP), and for individual GP sites. The AUC and optimal distance cutoffs are shown in each panel. For all GP sites, an optimal cutoff value of 11 mm was identified. Upper GP demonstrated lower cutoff values than lower GP, whereas site-specific analyses showed variable discriminatory performance depending on anatomic location. *P* values shown in each panel were derived from logistic regression models assessing the relationship between PV–GP distance and GP modification. ARGP = anterior right GP; AUC = area under the curve; GP = ganglionated plexus; ILGP = inferior left GP; IRGP = inferior right GP; MTGP = Marshall tract GP; PV = pulmonary vein; ROC = receiver operating characteristic; SLGP = superior left GP.

of 137); SLGP, 95.8% (69 of 72); MTGP, 98.1% (51 of 52); IRGP, 98.9% (86 of 87); and ILGP, 100.0% (67 of 67). These results confirmed that voltage mapping has strong agreement with HFS for assessing GP modification.

Multivariate analysis

Logistic regression analysis was performed to identify predictors of GP modification. The results are presented in Table 4. Univariate analysis identified PV–GP distance as a significant predictor of GP modification (odds ratio 0.68; 95% confidence interval 0.63–0.72; $P < .001$) but not LA volume, age, $CHADS_2$ score, sex, and mean body mass index. The multivariate models consistently identified PV–GP distance as an independent predictor of GP modification, with shorter distances being associated with higher modification rates (all $P < .001$). Other factors, including LA volume, age, and $CHADS_2$ score, were not found to be significant predictors. Overall, the PV–GP distance was the only

Table 3 Concordance between HFS and voltage mapping in 28 patients

Evaluation item	ARGP	SLGP	MTGP	IRGP	ILGP	Total
No. of GP-positive sites before CBA	137	72	52	87	67	415
No. of discrepancies between HFS and voltage after CBA	13	3	1	1	0	18
No. of consistencies between HFS and voltage after CBA	124	69	51	86	67	397
Consistency rate	90.5%	95.8%	98.1%	98.9%	100.0%	95.7%

Agreement between functional assessment using HFS and anatomic assessment using voltage mapping. The number of GP-positive sites before ablation, concordant and discordant findings after ablation, and consistency rates are shown for each region.

ARGP = anterior right GP; CBA = cryoballoon ablation; GP = ganglionated plexus; HFS = high-frequency stimulation; ILGP = inferior left GP; IRGP = inferior right GP; MTGP = Marshall tract GP; SLGP = superior left GP.

Table 4 Logistic regression analysis identifying predictors of GP modification

Variable	Univariate OR (95% CI)	*P* value	Model 1 OR (95% CI)	*P* value	Model 2 OR (95% CI)	*P* value	Model 3 OR (95% CI)	*P* value
PV–GP distance (mm)	0.68 (0.63–0.72)	<.001	0.68 (0.63–0.72)	<.001	0.68 (0.63–0.72)	<.001	0.68 (0.63–0.72)	<.001
Left atrial volume (mL)	1.00 (0.99–1.00)	.43	1.00 (0.99–1.01)	.83	1.00 (0.99–1.01)	.83	1.00 (0.99–1.01)	.63
Age (per 1-y increase)	1.01 (0.99–1.03)	.38			1.00 (0.97–1.03)	.83	1.00 (0.96–1.02)	.58
$CHADS_2$ score	1.05 (0.92–1.21)	.46					1.27 (0.94–1.73)	.12
Sex (male vs female)	1.07 (0.77–1.50)	.67						
BMI (kg/m^2)	1.02 (0.97–1.07)	.44						

Results of univariate and multivariate logistic regression analyses evaluating clinical and anatomic predictors of GP modification after cryoballoon ablation. Multivariate models included PV–GP distance with incremental adjustment for left atrial volume (model 1), age (model 2), and $CHADS_2$ score (model 3).

BMI = body mass index; $CHADS_2$ = congestive heart failure, hypertension, age, diabetes mellitus, and stroke/transient ischemic attack; CI = confidence interval; GP = ganglionated plexus; OR = odds ratio; PV–GP = pulmonary vein–ganglionated plexus.

consistent independent predictor of incidental GP modification after standard CBA. Adding other clinical variables did not improve the predictive accuracy. This result suggests that the PV–GP distance measured on the integrated EnSite–CT model can predict the extent of GP modification after CBA with high accuracy

Discussion

This study demonstrated a clear relationship between PV–GP distance and the extent of GP modification achieved by CBA. Our findings provide quantitative evidence that anatomic proximity is the primary determinant of incidental GP modification, with an overall optimal cutoff of 11 mm identified by ROC analysis. Notably, upper GP regions were effectively modified at shorter distances, 7–9 mm, whereas lower GP regions were rarely modified when the distances exceeded approximately 13 mm. Shorter PV–GP distance was associated with successful GP modification during CBA, as illustrated in the central illustration.

The SLGP and ARGP, located adjacent to the PV–LA junction, are known to contribute to AF initiation via autonomic stimulation,[7] and their anatomic location favors effective cryothermal energy delivery. In contrast, the IRGP and ILGP are located along the lower posterior LA and are more distant from the PV–LA junction, limiting effective cryothermal energy. The MTGP, embedded within the ligament of Marshall and involved in intrinsic cardiac autonomic regulation,[9] showed high modification rates owing to its proximity to the PV–LA junction, although anatomic variability may influence energy penetration. Hou et al[28] reported that the IRGP receives input from the ARGP and SLGP and functions as an integrative center regulating atrioventricular node activity. Furthermore, Po et al[18] demonstrated that IRGP ablation can prevents vagal nerve responses even during HFS at other GPs, supporting its central role within the atrial autonomic network. Although the ILGP is not considered an integrative center, interconnections among all GPs indicate that incomplete modification of the inferior GP may contribute to AF recurrence.[15] From a technical standpoint, the IRGP and ILGP are located in close proximity to the left inferior and right inferior PVs, regions in which CBA is technically challenging. As a result, incomplete balloon occlusion has been frequently observed, and adjunctive techniques, such as the pull-down maneuver, are often required to achieve sufficient coverage.[29,30] These technical limitations provide a mechanistic explanation for the lower modification rates observed at inferior GP sites. Moreover, these structural considerations offer a coherent explanation for the differences in the modification rates observed in this study. Following the criteria of Calò et al,[27] the current study defined voltage attenuation as <0.05 mV. This threshold effectively excludes background noise and provides a clinically meaningful standard for assessing GP modification.

Clinical implications and selection of energy source

The present findings suggest that PV–GP distance may provide a practical framework for identifying GP sites that are likely to be modified by CBA alone and those in which its effect may be limited. Upper GP sites located within approximately 7–9 mm of the PV–LA junction were frequently modified, whereas inferior GP sites located beyond approximately 13 mm were less likely to be modified. Thus, adjunctive mapping or ablation, including RF ablation, may be selectively considered when GP modification is clinically intended, particularly for distant inferior GP sites. However, evidence supporting combined cryoballoon and RF strategies remains limited,[19,31] and our findings should not be interpreted as recommending routine adjunctive ablation. HFS remains important for functional GP identification but requires an additional RF catheter during cryoballoon procedures, increasing procedural complexity and cost. PV–GP distance derived from preprocedural imaging, together with postablation voltage mapping, may provide complementary information for assessing GP modification, particularly in centers that do not routinely perform HFS. Future AF ablation strategies may integrate anatomic distance, functional testing, voltage mapping, and energy-source characteristics to guide selective autonomic modification.[32–35]

Limitations

This study has several notable limitations. First, this study was a single-center, retrospective analysis with a relatively small cohort of 50 patients. As such, the statistical power was limited, and the generalizability of the findings should be interpreted with caution. Thus, further studies with larger cohorts are required to validate the site-specific observations for each GP. Second, GP modification was defined by postablation voltage attenuation to <0.05 mV on voltage mapping. Although this threshold was derived from established electrophysiological criteria, it remains an indirect marker and lacks histologic corroboration. HFS validation was performed in 28 patients and showed high concordance; however, the number of patients remains limited. These findings should be considered preliminary. Third, some patients underwent additional ablation procedures, including LA roof ablation and cavotricuspid isthmus line ablation, after CBA and voltage mapping/HFS assessment. Consequently, the long-term durability of GP modification and its direct contribution to the suppression of AF recurrence could not be fully evaluated. Furthermore, the accuracy of distance measurements obtained by integrating CT images into the EnSite system, as well as the potential influence of interindividual anatomic variability, was not comprehensively evaluated. Although all procedures were performed using a 28 mm cryoballoon, technical parameters, such as contact pressure and freeze duration, were not systematically analyzed.

Taken together, these limitations suggest that the ability of the PV–GP distance to predict GP modification observed in this study should be regarded as exploratory. Future prospective multicenter investigations will be necessary to validate these findings and clarify their association with long-term clinical outcomes.

Conclusion

The current study provides quantitative evidence that the distance from the PV–LA junction to each HFS-defined GP site is the primary determinant of successful GP modification during CBA. As such, PV–GP distance measured on the integrated EnSite–CT model can be considered a practical tool for procedural planning, whereas voltage mapping provides an objective method for evaluating modification. These findings may serve as a useful reference for centers where HFS is not routinely performed.

Acknowledgments

We thank Marin Murakami and Takuya Taniguchi, clinical engineers at Osaka Prefecture Saiseikai Izuo Hospital, for assistance with data collection. We also thank Mr Tomohiro Kasu of Nihon Kohden Corporation for support with data processing. Finally, we thank Dr Yumie Matsui, formerly of our institution until 2023, for her guidance and contributions to this study and manuscript preparation.

Funding Sources: This research did not receive any specific grant from funding agencies in the public, commercial, or not-for-profit sectors.

Disclosures: The authors have no conflicts of interest to disclose.

Authorship: All authors attest they meet the current ICMJE criteria for authorship.

Patient Consent: An informed consent was obtained through an opt-out process in accordance with institutional and national ethics guidelines.

Ethics Statement: The study protocol was reviewed and approved by the Ethics Committee of Osaka Prefecture Saiseikai Izuo Hospital on August 19, 2024.

Data availability: The data are not publicly available owing to patient privacy and institutional policy, but are available from the corresponding author on reasonable request.

References

1. Chung SC, Sofat R, Acosta-Mena D, et al. Atrial fibrillation epidemiology, disparity and healthcare contacts: a population-wide study of 5.6 million individuals. Lancet Reg Health Eur 2021;7:100157.
2. Benjamin EJ, Muntner P, Alonso A, et al. Heart disease and stroke statistics-2019 update: a report from the American Heart Association. Circulation 2019; 139:e56–e528.
3. Haïssaguerre M, Jaïs P, Shah DC, et al. Spontaneous initiation of atrial fibrillation by ectopic beats originating in the pulmonary veins. N Engl J Med 1998; 339:659–666.
4. Van Belle Y, Janse P, Rivero-Ayerza MJ, et al. Pulmonary vein isolation using an occluding cryoballoon for circumferential ablation: feasibility, complications, and short-term outcome. Eur Heart J 2007;28:2231–2237.
5. Packer DL, Kowal RC, Wheelan KR, et al. Cryoballoon ablation of pulmonary veins for paroxysmal atrial fibrillation: first results of the North American Arctic Front (STOP AF) pivotal trial. J Am Coll Cardiol 2013;61:1713–1723.
6. Kuck KH, Brugada J, Fürnkranz A, et al. Cryoballoon or radiofrequency ablation for paroxysmal atrial fibrillation. N Engl J Med 2016;374:2235–2245.
7. Scherlag BJ, Nakagawa H, Jackman WM, et al. Electrical stimulation to identify neural elements on the heart: their role in atrial fibrillation. J Interv Card Electrophysiol 2005;13:37–42.
8. Lemery R, Birnie D, Tang ASL, Green M, Gollob M. Feasibility study of endocardial mapping of ganglionated plexuses during catheter ablation of atrial fibrillation. Heart Rhythm 2006;3:387–396.
9. Katritsis DG, Giazitzoglou E, Zografos T, Pokushalov E, Po SS, Camm AJ. Rapid pulmonary vein isolation combined with autonomic ganglia modification: a randomized study. Heart Rhythm 2011;8:672–678.
10. Choi EK, Shen MJ, Han S, et al. Intrinsic cardiac nerve activity and paroxysmal atrial tachyarrhythmia in ambulatory dogs. Circulation 2010;121:2615–2623.
11. Bettoni M, Zimmermann M. Autonomic tone variations before the onset of paroxysmal atrial fibrillation. Circulation 2002;105:2753–2759.
12. Hou Y, Scherlag BJ, Lin J, et al. Ganglionated plexi modulate extrinsic cardiac autonomic nerve input. J Am Coll Cardiol 2007;50:61–68.
13. Po SS, Scherlag BJ, Yamanashi WS, et al. Experimental model for paroxysmal atrial fibrillation arising at the pulmonary vein–atrial junctions. Heart Rhythm 2006;3:201–208.
14. Stavrakis S, Nakagawa H, Po SS, Scherlag BJ, Lazzara R, Jackman WM. The role of the autonomic ganglia in atrial fibrillation. JACC Clin Electrophysiol 2015;1:1–13.
15. Nakagawa H, Scherlag BJ, Patterson E, Ikeda A, Lockwood D, Jackman WM. Pathophysiologic basis of autonomic ganglionated plexus ablation in patients with atrial fibrillation. Heart Rhythm 2009;6:S26–S34.
16. Pokushalov E, Romanov A, Shugayev P, et al. Selective ganglionated plexi ablation for paroxysmal atrial fibrillation. Heart Rhythm 2009;6:1257–1264.
17. Pokushalov E, Romanov A, Artyomenko S, Turov A, Shirokova N, Katritsis DG. Left atrial ablation at the anatomic areas of ganglionated plexi for paroxysmal atrial fibrillation. Pacing Clin Electrophysiol 2010;33:1231–1238.
18. Po SS, Nakagawa H, Jackman WM. Localization of left atrial ganglionated plexi in patients with atrial fibrillation: techniques and technology. J Cardiovasc Electrophysiol 2009;20:1186–1189.
19. Pokushalov E, Romanov A, Artyomenko S, et al. Ganglionated plexi ablation for longstanding persistent atrial fibrillation. Europace 2010;12:342–346.
20. Garabelli P, Stavrakis S, Kenney JFA, Po SS. Effect of 28-mm cryoballoon ablation on major atrial ganglionated plexi. JACC Clin Electrophysiol 2018;4:831–838.
21. Peyrol M, Barraud J, Koutbi L, et al. Vagal reactions during cryoballoon-based pulmonary vein isolation: a clue for autonomic nervous system modulation? BioMed Res Int 2016;2016:7286074.

22. Herweg B, Patel RS, Noujaim S, Spano J, Mencer N, Vijayaraman P. Cryoballoon cardioneuroablation: new electrophysiological insights. Heart Rhythm 2024;5:209–216. O2.
23. Yorgun H, Aytemir K, Canpolat U, Şahiner L, Kaya EB, Oto A. Additional benefit of cryoballoon-based atrial fibrillation ablation beyond pulmonary vein isolation: modification of ganglionated plexi. Europace 2014;16:645–651.
24. Nademanee K, McKenzie J, Kosar E, et al. A new approach for catheter ablation of atrial fibrillation: mapping of the electrophysiologic substrate. J Am Coll Cardiol 2004;43:2044–2053.
25. Rolf S, Kircher S, Arya A, et al. Tailored atrial substrate modification based on low-voltage areas in catheter ablation of atrial fibrillation. Circ Arrhythm Electrophysiol 2014;7:825–833.
26. Estner HL, Deisenhofer I, Luik A, et al. Electrical isolation of pulmonary veins in patients with atrial fibrillation: reduction of fluoroscopy exposure and procedure duration by the use of a non-fluoroscopic navigation system (NavX). Europace 2006;8:583–587.
27. Calò L, Rebecchi M, Sciarra L, et al. Catheter ablation of right atrial ganglionated plexi in patients with vagal paroxysmal atrial fibrillation. Circ Arrhythm Electrophysiol 2012;5:22–31.
28. Hou Y, Scherlag BJ, Lin J, et al. Interactive atrial neural network: determining the connections between ganglionated plexi. Heart Rhythm 2007;4:56–63.
29. Yasuoka R, Kurita T, Kotake Y, et al. Particular morphology of inferior pulmonary veins and difficulty of cryoballoon ablation in patients with paroxysmal atrial fibrillation. Circ J 2017;81:668–674.
30. Andrade JG. Cryoablation for atrial fibrillation. Heart Rhythm 2020;1:44–58. O2.
31. Katritsis DG, Pokushalov E, Romanov A, et al. Autonomic denervation added to pulmonary vein isolation for paroxysmal atrial fibrillation: a randomized clinical trial. J Am Coll Cardiol 2013;62:2318–2325.
32. Reddy VY, Neuzil P, Koruth JS, et al. Pulsed field ablation for pulmonary vein isolation in atrial fibrillation. J Am Coll Cardiol 2019;74:315–326.
33. Musikantow DR, Neuzil P, Petru J, et al. Pulsed field ablation to treat atrial fibrillation: autonomic nervous system effects. JACC Clin Electrophysiol 2023;9:481–493.
34. Gerstenfeld EP, Mansour M, Whang W, et al. Autonomic effects of pulsed field vs thermal ablation for treating atrial fibrillation: subanalysis of advent. JACC Clin Electrophysiol 2024;10:1634–1644.
35. Anter E, Mansour M, Nair DG, et al. Dual-energy lattice-tip ablation system for persistent atrial fibrillation: a randomized trial. Nat Med 2024;30:2303–2310.